

## Case Report

# Corticobasal degeneration with deep white matter lesion diagnosed by brain biopsy

**Akira Arakawa,<sup>1</sup>  Yuko Saito,<sup>2</sup> Tomonari Seki,<sup>1</sup> Akihiko Mitsutake,<sup>1</sup> Tatsuya Sato,<sup>1</sup> Junko Katsumata,<sup>1</sup> Risa Maekawa,<sup>1</sup> Takuto Hideyama,<sup>1</sup> Koichi Tamura,<sup>3</sup> Masato Hasegawa<sup>4</sup> and Yasushi Shiio<sup>1</sup>**

Departments of <sup>1</sup>Neurology, <sup>3</sup>Pathology, Tokyo Teishin Hospital, <sup>2</sup>Department of Pathology and Laboratory Medicine, National Center Hospital, National Center of Neurology and Psychiatry and <sup>4</sup>Department of Dementia and Higher Brain Function, Metropolitan Institute of Medical Science, Tokyo, Japan

**Corticobasal degeneration (CBD)** is a rare progressive neurodegenerative disorder characterized by asymmetric presentation of cerebral cortex signs, cortical sensory disturbance and extrapyramidal signs. Herein, we report a case of a 66-year-old Japanese woman who presented with apraxia of the right hand. She subsequently developed postural instability and cognitive impairments that rapidly worsened. One and a half years later, the patient was wheelchair-bound and severely demented. Brain magnetic resonance imaging revealed left dominant atrophy of the frontoparietal lobe. There was a hyperintense lesion in the deep white matter expanding toward the subcortical area on fluid-attenuated inversion recovery (FLAIR) images. In order to rule out the possibility of an intracranial tumor such as an astrocytoma or malignant lymphoma, we performed a brain biopsy of the left frontal middle gyrus. The patient became bedridden and showed akinetic mutism 1 year after biopsy. Pathological examination revealed a large amount of 4-repeat tau-immunoreactive neuropil threads scattered predominantly in the corticomedullary junction and tau-immunoreactive structures, consistent with CBD. Immunostaining for p53 showed no positive cells, and there were very few Ki-67-positive cells. On immunoblots of sarkosyl-insoluble brain extracts, a major doublet of 64 and 68 kDa full-length tau with two closely related fragments of approximately 37 kDa were detected. Based on these results, the patient was pathologically diagnosed as having CBD, excluding the possibility of tumor. Taken together with previous similar case reports, our findings indicate that a deep white matter hyperintense lesion

on FLAIR images may be a useful clue to CBD, predicting rapid clinical progression with severe dementia based on severe white matter degeneration with a large amount of tau accumulation on pathological examination.

**Key words:** dementia, frontotemporal dementia, neuropil threads, tau proteins, white matter.

## INTRODUCTION

Corticobasal degeneration (CBD) is a slowly progressive neurodegenerative disorder first reported by Rebeiz *et al.* in 1968.<sup>1</sup> The characteristic clinical presentations include asymmetric presentation of enhanced tendon reflex, positive planter reflection, apraxia, cortical sensory disturbance and levodopa-resistant parkinsonism. However, some neurodegenerative disorders such as Alzheimer's disease, Pick's disease, and progressive supranuclear palsy present with a CBD-like clinical picture. Therefore, the term "corticobasal syndrome (CBS)" is used to represent such a clinical picture.<sup>2</sup> In addition, since pathologically diagnosed CBD cases occasionally present with clinical pictures similar to Alzheimer-type dementia, progressive supranuclear palsy, and frontotemporal dementia, CBD is now used as a pathological diagnostic term.<sup>3</sup>

CBD is pathologically characterized by neuronal loss and gliosis in the cerebral cortex and various subcortical nuclei. Degeneration of the cerebral white matter is also observed.<sup>4</sup> Another pathological finding is abnormal tau accumulation in both neurons and glia, including pretangles, ballooned neurons and astrocytic plaques in the cerebral cortex and subcortical nuclei, and neuropil threads and coiled bodies in the white matter.<sup>5</sup> These structures are composed of 4-repeat (4R) tau, a tau isoform. Therefore, CBD is classified as a 4R tauopathy.<sup>6</sup>

On brain magnetic resonance imaging (MRI), CBD is characterized by asymmetric cortical atrophy of the frontoparietal lobe.<sup>7</sup> In addition, CBD patients occasionally show subcortical white matter hyperintense lesions, which are usually observed

Correspondence: Akira Arakawa, MD, Department of Neurology, Tokyo Teishin Hospital, Tokyo Fujimi 2-14-23, Chiyoda-ku, Tokyo 102-0071, Japan. Email: aarakawa-tyk@umin.ac.jp

Received 27 September 2019; revised and accepted 07 December 2019.

beneath the affected area on fluid-attenuated inversion recovery (FLAIR) images.<sup>8-12</sup> The underlying pathophysiology is still controversial, although several studies suggest the progression of neuronal degeneration,<sup>8-10</sup> or the accumulation of abnormally phosphorylated tau in oligodendroglia,<sup>11,12</sup> contribute to the signal change in MRI. In addition, deep white matter hyperintense lesions were also described in some CBD patients.<sup>11,12</sup>

In this study, we report a biopsied case of pathologically diagnosed CBD. Clinical progression occurred more rapidly than typical CBD cases and was accompanied by severe dementia. This case was significant because it highlighted the possibility that deep white matter hyperintense lesions on FLAIR images represent a clue to CBD, predicting rapid clinical progression with severe dementia.

### CLINICAL SUMMARY

The patient's growth and development were normal. Her parents had a history of dementia, but clinical details were not obtained. The patient first noticed difficulty

performing her daily work, such as dining and writing, at the age of 65. These symptoms worsened, and half a year later, she was referred to our department. Upon neurological examination, we observed parkinsonism (rigidity and akinesia) and apraxia predominantly on the right side. Mild cognitive impairment was also evident. Brain MRI revealed mild cortical atrophy in the left frontoparietal lobe, which was most prominent around the central sulcus. In addition, hyperintense lesions were present in the deep white matter of the frontoparietal lobe on FLAIR images (Fig. 1A, B). We diagnosed the patient as CBS, and decided to follow-up as an outpatient.

At the age of 66, 1 year later from first admission, she was admitted to our hospital for further examination. By this time, her gait disturbance and cognitive impairment had worsened, and she also presented with apathy and irritability. She had begun falling frequently because of postural instability and had started using a wheelchair. Neurological examination revealed severe dementia (she could not even tell us her name), frontal executive dysfunction (apathy, irritability and forced grasping), and limb-kinetic apraxia. We observed

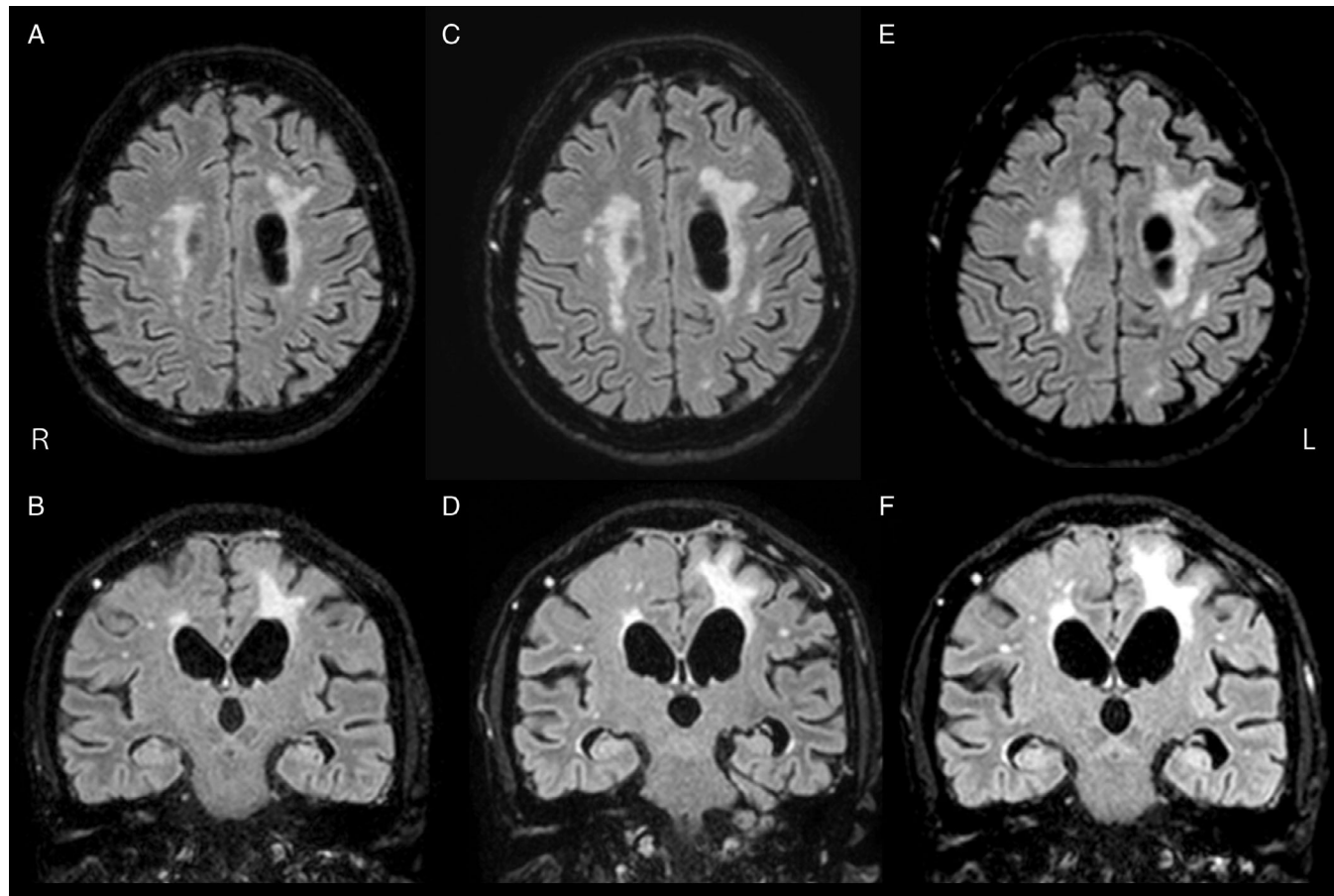


**Fig. 1** FLAIR images by MRI. Asymmetric, progressive atrophy (right < left) of the frontal and parietal lobes, which is most dominant near the central sulcus, is evident. Slightly progressive ventricular dilatation is also observed. An asymmetric hyperintense (right < left) lesion in the deep white matter is gradually expanding toward the subcortical lesion. Panels (A, B), (C, D) and (E, F) indicate images obtained at 6, 10 and 15 months, respectively, after onset.

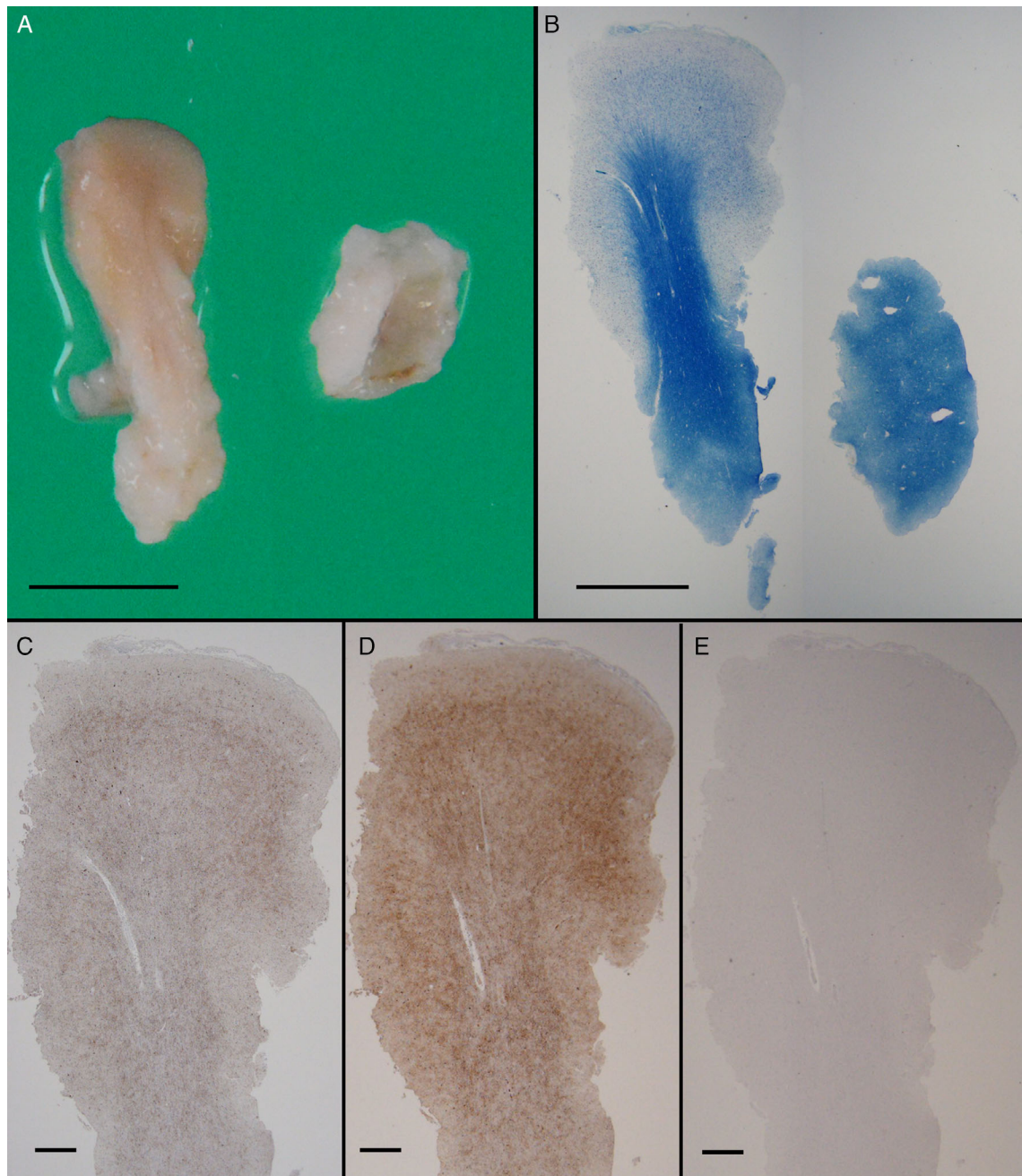


**Fig. 2** Macroscopic and semimicroscopic findings of the specimen, showing brownish-tan discoloration in the cortex and subcortical white matter (A), mild-to-moderate myelin pallor in the deep white matter (B), 4R-tau accumulation in the corticomedullary junction (B), and areas immunopositive for phosphorylated tau by AT8 (C), immunopositive for 4R-tau by RD4 (D) and immunonegative for 3R-tau by RD4 (E). KB staining (B), immunohistochemical staining (C-E). Scale bars: 5 mm (A), 2 mm (B), 500  $\mu$ m (C-E).

weakness, hyperreflexia, and positive planter reflexions in her right limbs. Dystonia was seen in her right arm, fixed in the flexor position. Extrapyramidal signs, including cog-wheel rigidity and akinesia, were observed predominantly in the right arm, and these symptoms did not respond to levodopa treatment (up to 600 mg/day). Vertical gaze palsy and nystagmus were not observed. Since frontotemporal dementia with parkinsonism linked to chromosome 17 occasionally

present with CBS,<sup>13</sup> we performed Sanger sequencing of the microtubule-associated protein tau (MAPT) gene (*MAPT*), which revealed no mutations.

On FLAIR images by brain MRI, we found that her frontoparietal lobe atrophy had progressed. White matter lesions were expanding toward the subcortical area, which did not show gadolinium enhancement (Fig. 1 C, D: 10 months after onset; E, F: 15 months after onset). <sup>123</sup>I-

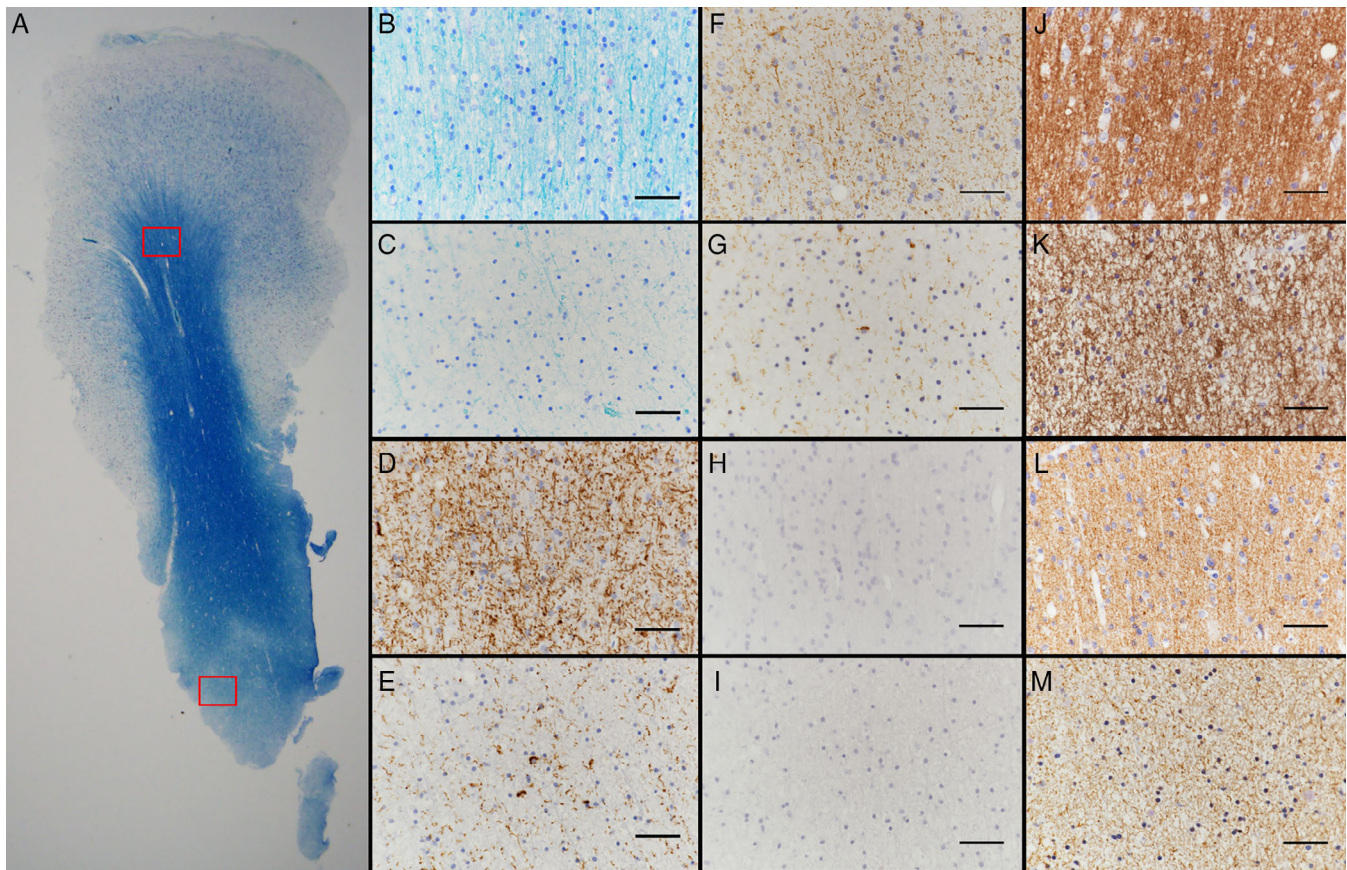


**Fig. 3** Semimacroscopic (A) and microscopic (B–M) findings in the subcortical and deep white matter lesion. Semimacroscopic (A) and microscopic (B, C) examination on KB-stained sections reveals myelin pallor in the deep white matter. Microscopic examination reveals 4R-tau (RD4) immunoreactivity seems to be less intense in the lesion (D–E). Although lower amounts of phosphorylated tau (AT8)-positive structures are scattered, the same tendency is observed (F, G). No apparent 3R-tau (RD3)-positive structures are observed (H, I). The same tendency is observed by immunohistochemical staining for myelin basic protein (J, K) and phosphorylated neurofilament protein (L, M). Scale bars: 2 mm (A), 50  $\mu$ m (B–M).

N-3-fluoropropyl-2 $\beta$ -carbomethoxy-3 $\beta$ -4-iodophenyl tropane ( $^{123}\text{I}$ -FP-CIT) dopamine transporter (DAT)-single photon emission computed tomography (SPECT) (DAT-SPECT) revealed reduced striatum accumulation, which was more prominent on the left side. Specific binding ratio was decreased to 1.43 on the left and 2.41 on the right side (lower limit: 4.50).

These clinical and radiological findings were compatible with CBS. However, we could not exclude the possibility that the expanding hyperintense lesion in the deep white matter on FLAIR images and her rapid cognitive deterioration reflected an intracranial tumor such as astrocytoma or malignant lymphoma. So, we performed further laboratory and radiological examinations.

As for laboratory examinations, serum-soluble interleukin-2 receptor, tumor markers (carcinoembryonic antigen, carbohydrate antigen 19-9, carbohydrate antigen 125 and gastrin-releasing peptide) were within normal range. Cerebrospinal fluid examination showed normal level of cells (1/ $\mu$ L), glucose (58, 98 mg/dL in serum) and protein (30 mg/dL).

Cytology was class I. Truncal CT revealed no mass lesion, including swollen lymph nodes.  $\text{Tc-99m}$ -ethyl cysteinate dimer (ECD)-SPECT ( $\text{Tc-99m}$  ECD-SPECT) revealed hypoperfusion areas in the left frontoparietal lobe with no abnormal hyperperfusion areas in the cerebrum.

After open biopsy was performed, the patient was discharged without any complication. However, postural instability, cognitive impairment were further exacerbated. The patient became bedridden with akinetic mutism 1 year after biopsy, and admitted to a chronic care hospital as a long-period hospitalized patient.

## PATHOLOGICAL FINDINGS

After obtaining written informed consent from the patient and family members, we performed an open biopsy from the left middle frontal gyrus. The specimen consisted of two pieces. One was 15  $\times$  5 mm in size with gray and white matter, and the other was 5  $\times$  5 mm in size with white matter. Considering the size of the specimen, we speculate that

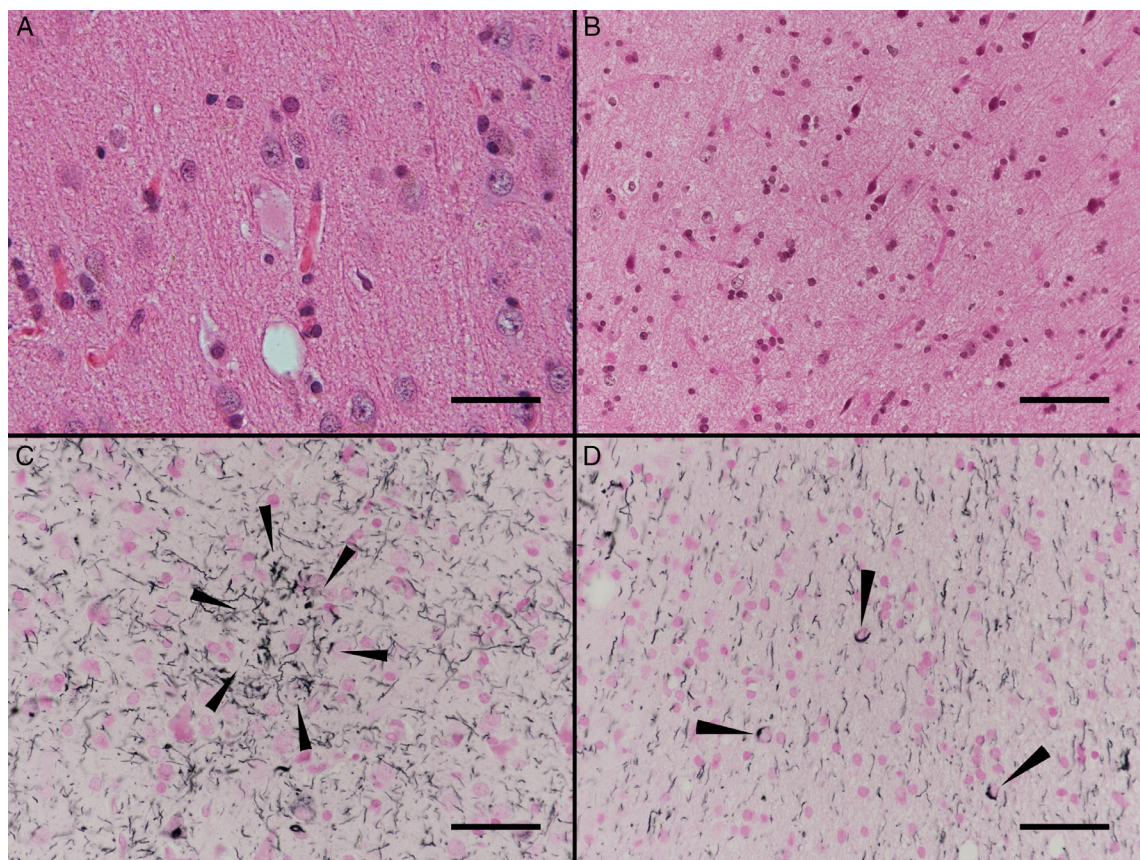


**Fig. 4** Microphotographs of the biopsy specimen sections stained with HE (A, B) and Gallyas-Braak (C, D). In the cerebral cortex, ballooned neurons (A), gliotic and rarefactive changes (B), astrocytic plaques (C, arrowheads), and coiled bodies (D, arrowheads) are observed. Scale bars: 35  $\mu$ m (A), 50  $\mu$ m (B, C, D).

the specimen did not exactly involve the deep matter lesion where signal change by MRI was first observed. Both pieces were fixed for 48 h in 4% paraformaldehyde in 100 mM phosphate buffer, pH 7.4 and subsequently embedded in paraffin. A small portion of each piece was embedded with 20% formaldehyde for 48 h and embedded in paraffin. Slices were cut at a thickness of 6  $\mu$ m and stained with hematoxylin and eosin (HE), Klüver-Barrera (KB), and Gallyas-Braak methods for routine pathological examination. The paraffin-embedded sections were immunostained with an automated immunostainer (Ventana XT DISCOVERY; Roche, Tokyo, Japan), as previously described in detail.<sup>14</sup> For the diagnosis of CBD, the primary antibodies against phosphorylated tau (monoclonal, AT8; Innogenetics, Temse, Belgium), 3R-tau (monoclonal, clone RD3; Upstate, Lake Placid, NY, USA), and 4R-tau (monoclonal, clone RD4; Upstate). For the exclusion of malignant tumor, we used the primary antibodies against myelin basic protein (polyclonal; Dako, Glostrup, Denmark), phosphorylated neurofilament protein (monoclonal, clone SMI31; Sternberger Monoclonals, Lutherville, MD, USA), Ki-67

(monoclonal, clone MIB-1; Dako), and p53 (monoclonal, clone M3626; Dako).

Extraction of sarkosyl-insoluble tau, electrophoresis and immunoblotting were performed as previously described.<sup>15</sup> The primary antibody used was T46 (ThermoFisher Scientific, Rockford, IL, USA), which recognizes the C-terminal region of tau.

Upon macroscopic and semimicroscopic examination of the biopsy, we observed a brownish-tan discoloration around the corticomedullary junction and thinning of the cortex (Fig. 2A). KB staining showed mild-to-moderate myelin loss, which was more prominent in the deep lesion of the specimen. Focal demyelination was not observed (Fig. 2B). Immunohistochemical staining for phosphorylated tau (Fig. 2C), 3R-tau (Fig. 2D), and 4R-tau (Fig. 2E) revealed a large amount of 4R-positive, phosphorylated tau-positive structures scattered predominantly in the gray and white matter at the corticomedullary junction.

Regarding myelin pallor in the deep white matter of the specimen, 4R-tau seemed to be less accumulated in that lesion (Fig. 3A). This tendency was more prominent on microscopic observation (Fig. 3B–E). Although less

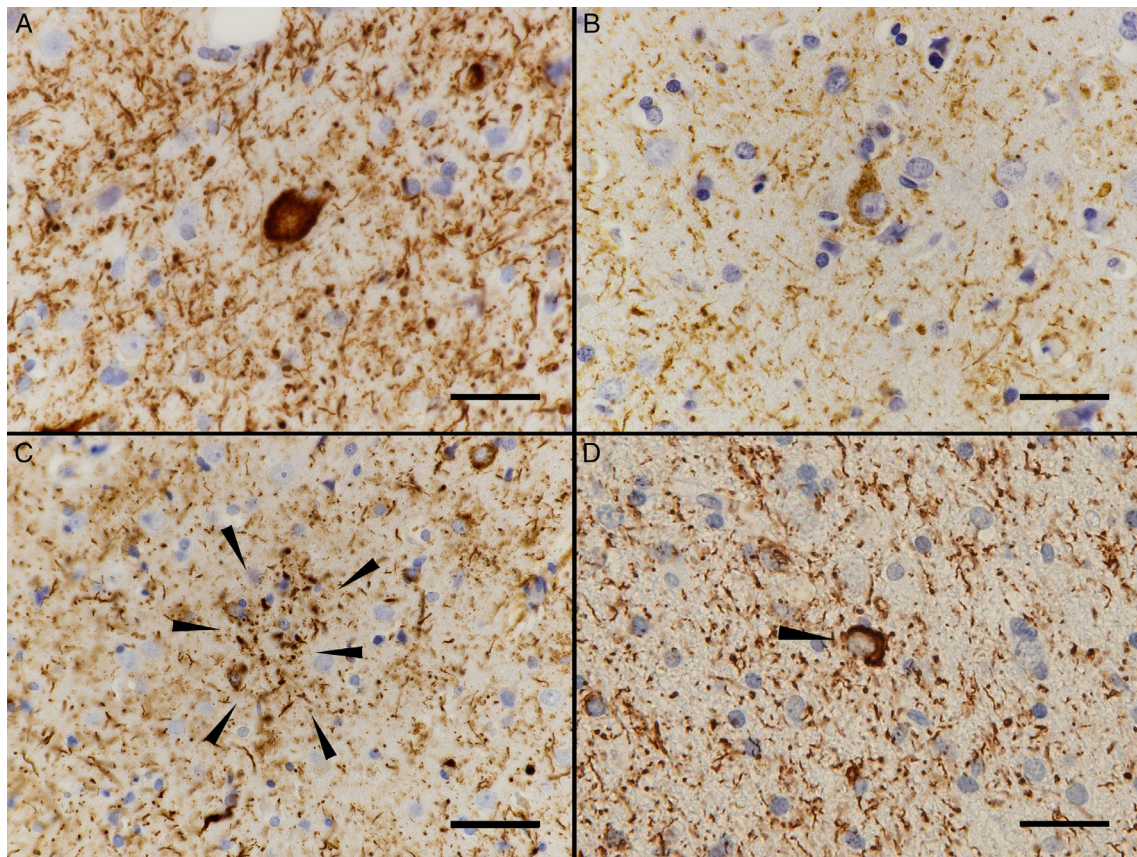


**Fig. 5** Microphotographs of the biopsy specimen sections immunostained for phosphorylated tau by AT8 (A, D) and 4R-tau by RD4 (B, C). A ballooned neuron (A), a pretangle (B), an astrocytic plaque (C), and a coiled body (D) are observed. Scale bars: 30  $\mu$ m (A-D).

**Table 1** Clinical and MRI findings of pathologically diagnosed CBD with deep white matter hyperintense lesions on FLAIR images

	Onset (year)	Sex	Duration (year)	Cortical syndrome	Dementia	Clinical diagnosis	Atrophy and white matter lesion on FLAIR	Genetic analysis of tau gene
Case 1 <sup>11</sup>	67	M	3	No sign	Severe	PDD	Lt. frontoparietal	N/A
Case 2 <sup>12</sup>	59	F	6	Apraxia	Severe	PiD	Lt. frontotemporal	No mutation
Case 3 <sup>12</sup>	62	M	5	Alien hand sign	Severe	CBS	Rt. frontoparietal	No mutation
This case	65	F	1.5 <sup>†</sup>	Apraxia	Severe	CBS	Lt. frontoparietal	No mutation

CBS, corticobasal syndrome; FLAIR, fluid-attenuated inversion recovery; Lt, left; PDD, Parkinson disease with dementia; PiD, Pick's disease; Rt, right. <sup>†</sup>The duration from onset to biopsy.

amounts of phosphorylated tau-positive structures was scattered, the same tendency was observed (Fig. 3F–G). No apparent RD-3 positive structures were observed (Fig. 3H–I). In addition to decreased myelin, the number of axons was decreased in the deep side of the white matter (Fig. 3J–M).

Using HE staining we microscopically observed ballooned neurons (Fig. 4A), as well as mild neuronal loss with gliosis and rarefaction in the cortex (Fig. 4B). No atypical cells, lymphocyte infiltration, or inclusion bodies were observed. Gallyas-Braak staining revealed pretangles and astrocytic plaques in the cortex (Fig. 4C,

black arrowheads), as well as coiled bodies in both gray and white matter (Fig. 4D, black arrowheads). A large number of neuropil threads were observed at the corticomedullary junction. High magnification images of tau immunostaining in the cortex revealed many tau-positive ballooned neurons (Fig. 5A), pretangles (Fig. 5B), astrocytic plaques (Fig. 5C, black arrowheads), and coiled bodies (Fig. 5D, black arrowhead). These astrocytic plaques were formed differently compared to those in typical CBD cases. Immunostaining for p53 showed no positive cells, and there were very few Ki-67-positive cells.

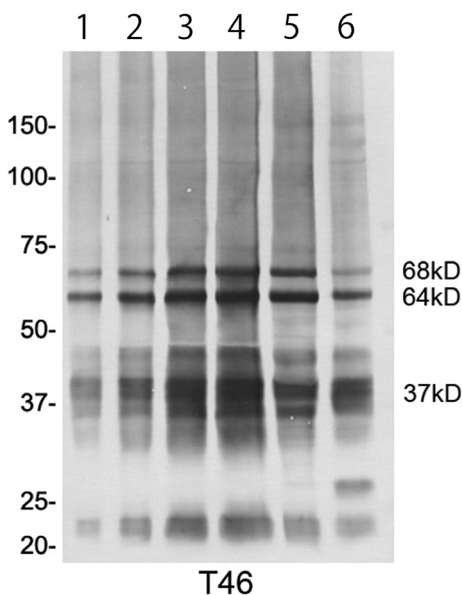


**Fig. 6** Immunoblot analysis of sarkosyl-insoluble tau from our case and typical CBD cases. The insoluble tau from our case is diluted at 1:20 (lane 1), 1:10 (lane 2), 1:5 (lane 3) and 1:3.3 (lane 4), and blotted with anti-tau antibody (T46). The electrophoretic mobility pattern of low molecular weight tau fragments of our case is consistent with that of typical CBD cases (lanes 5 and 6), particularly in two closely related prominent bands at 37 kDa. The antibody T46 recognizes the C-terminal region at amino acid residues 404–441 of human tau protein.

By immunoblotting of insoluble tau, a major doublet of 68 and 64 kDa, which correspond to hyperphosphorylated full-length 4R-tau isoforms, and C-terminal fragments of 37 kDa, were detected in our biopsied CBD case. The banded color of tau was so intense that dilution of the extracts was necessary to examine the banding pattern, which was indistinguishable from that of typical CBD autopsied cases<sup>16</sup> (Fig. 6).

These pathological findings are consistent with the neuropathologic criteria for CBD, which Dickson *et al.* proposed in 2002.<sup>5</sup> The possibility of tumor was ruled out.

## DISCUSSION

This is the first report to focus on the clinical and neuropathological findings of a CBD patient with a hyperintense lesion in the deep white matter on FLAIR images by brain MRI. The clinical course of our patient was rapid compared to typical CBD cases, and was accompanied by severe dementia in the early stages. Although MR spectroscopy could serve as a tool for differential diagnosis of malignant lymphoma or astrocytoma, the biopsy spared the effort of further invasive or non-invasive examination or confusion of differential diagnosis, and served for the prognostic prediction of this case. Most pathologically diagnosed CBD cases present with 6–8 years of disease

duration,<sup>17</sup> becoming wheelchair-bound 3–5 years after onset. In addition, although most CBD cases show variable degrees of cognitive impairment,<sup>18</sup> memory is usually preserved until the later stages.<sup>19</sup> At the time of brain biopsy, one and a half years from onset, our patient was wheelchair-bound, with severe frontal executive dysfunction and cognitive impairment. These findings suggest that her clinical progression, especially her cognitive deterioration, was rapid compared to typical CBD cases. Immunoblotting of sarkosyl-insoluble tau showed a banding pattern similar to previously autopsied cases,<sup>16</sup> which indicated that the 37 kDa tau fragments characteristic of CBD are generated during disease progression but not a post-mortem change.

Hyperintense lesions in the subcortical white matter on FLAIR images is occasionally observed in CBD cases.<sup>8–12</sup> By histopathological examination, areas overlapping with these hyperintense lesions contained myelin pallor and tau-positive structures.<sup>11</sup> Tau accumulation leads to metabolic alterations and subsequent death of oligodendroglial cells, contributing to white matter degeneration that may appear as a hyperintense lesion on FLAIR images.<sup>11,12</sup>

There were only two previous studies on pathologically diagnosed CBD cases showing hyperintense lesions in the deep white matter on FLAIR images.<sup>11,12</sup> We compared the clinical course and radiological characteristics of our case with previously reported CBD cases (Table 1). All four cases showed rapid clinical progression compared to typical CBD cases and presented with severe dementia in the early stage. On pathological examination, severely decreased myelin sheath staining in the white matter was observed in all autopsy cases. In addition, a large amount of tau accumulation was observed in the white matter in case 2, as observed in our case. In our case, atypical form of astrocytic plaques were observed, partly because of the numerous amount of tau accumulation. It is also possible that some difference in biochemical properties of tau protein underlies these atypical astrocytic plaques, which might be attributed to biopsy procedure. Genetic analysis of *MAPT* was performed in three cases (cases 2, 3 and our case), but no mutations were found.

These findings indicate that deep white matter hyperintense lesions on FLAIR images potentially reflect a new clue to CBD that predicts rapid clinical progression, severe dementia in the early stage of the disease, and a large amount of tau accumulation. The pathophysiological mechanism underlying the signal change in the deep white matter remains to be elucidated. Possible explanations include the following two points. First, in the deep white matter, a larger amount of tau is accumulated than in the subcortical white matter. Therefore the degeneration occurred more rapidly in the deep white matter, making tau accumulation less in the lesion. Second, tau

accumulation in the subcortical white matter and gray matter induces axonal degeneration and secondary myelin loss, making deep white matter more degenerated. A major limitation of this study is that the pathological findings of this case may not exactly reflect the findings in the deep white matter lesion since the specimen did not include the affected deep matter lesion, although tau accumulates less in the deep white matter than the subcortical white matter as far as we could observe. In addition, the pathological findings from patients affected with deep white matter lesions have not been well documented in previous reports. Further studies are necessary to understand the pathophysiological mechanism of deep white matter lesions.

## ACKNOWLEDGMENTS

The authors thank Dr. Makoto Noguchi and Dr. Madoka Hatasa for the biopsy, and Mr. Katsuyuki Umeto, Ms. Ayako Sato and Ms. Yoko Tanaka for technical support. This research was supported by AMED (grant number JP18dm0107103), Intramural Research Grant (30-8) for Neurological and Psychiatric Disorders of NCNP and JSPS KAKENHI (grant number JP 221S0003 and JP 16H06277 to Y. Saito).

## DISCLOSURE

The authors declare no conflict of interest.

## REFERENCES

1. Rebeiz JJ, Kolodny EH, Richardson EP Jr. Corticodentatonigral degeneration with neuronal achromasia. *Arch Neurol* 1968; **18**: 20–33.
2. Boeve BF, Lang AE, Litvan I. Corticobasal degeneration and its relationship to progressive supranuclear palsy and frontotemporal dementia. *Ann Neurol* 2003; **54**: S15–S19.
3. Armstrong MJ, Litvan I, Lang AE et al. Criteria for the diagnosis of corticobasal degeneration. *Neurology* 2013; **80**: 496–503.
4. Kondo D, Hino H, Shibuya K et al. An autopsied case of corticobasal degeneration showing severe cerebral atrophy over a protracted disease course of 16 years. *Neuropathology* 2015; **35**: 280–288.
5. Dickson DW, Bergeron C, Chin SS et al. Office of Rare Diseases neuropathologic criteria for corticobasal degeneration. *J Neuropathol Exp Neurol* 2002; **61**: 935–946.
6. Kouri N, Whitwell JL, Josephs KA, Rademakers R, Dickson DW. Corticobasal degeneration: A pathologically distinct 4R tauopathy. *Nat Rev Neurol* 2011; **7**: 263–272.
7. Josephs KA, Tang-Wai DF, Edland SD et al. Correlation between antemortem magnetic resonance imaging findings and pathologically confirmed corticobasal degeneration. *Arch Neurol* 2004; **61**: 1881–1884.
8. Tokumaru AM, O’uchi T, Kuru Y, Maki T, Murayama S, Horichi Y. Corticobasal degeneration: MR with histopathologic comparison. *AJNR Am J Neuroradiol* 1996; **17**: 1849–1852.
9. Doi T, Iwasa K, Makifuchi T, Takamori M. White matter hyperintensities on MRI in a patient with corticobasal degeneration. *Acta Neurol Scand* 1999; **99**: 199–201.
10. Koyama M, Yagishita A, Nakata Y, Hayashi M, Bandoh M, Mizutani T. Imaging of corticobasal degeneration syndrome. *Neuroradiology* 2007; **49**: 905–912.
11. Tokumaru AM, Saito Y, Murayama S et al. Imaging-pathologic correlation in corticobasal degeneration. *AJNR Am J Neuroradiol* 2009; **30**: 1884–1892.
12. Tan CF, Piao YS, Kakita A et al. Frontotemporal dementia with co-occurrence of astrocytic plaques and tufted astrocytes, and severe degeneration of the cerebral white matter: A variant of corticobasal degeneration? *Acta Neuropathol* 2005; **109**: 329–338.
13. Forrest SL, Kril JJ, Stevens CH et al. Retiring the term FTDP-17 as MAPT mutations are genetic forms of sporadic frontotemporal tauopathies. *Brain* 2018; **141**: 521–534.
14. Saito Y, Kawashima A, Ruberu NN et al. Accumulation of phosphorylated alpha-synuclein in aging human brain. *J Neuropathol Exp Neurol* 2003; **62**: 644–654.
15. Taniguchi-Watanabe S, Arai T, Kametani F et al. Biochemical classification of tauopathies by immunoblot, protein sequence and mass spectrometric analyses of sarkosyl-insoluble and trypsin-resistant tau. *Acta Neuropathol* 2006; **131**: 267–280.
16. Arai T, Ikeda K, Akiyama H et al. Identification of amino-terminally cleaved tau fragments that distinguish progressive supranuclear palsy from corticobasal degeneration. *Ann Neurol* 2004; **55**: 72–79.
17. Cairns NJ, Ghoshal N. FUS: A new actor on the frontotemporal lobar degeneration stage. *Neurology* 2010; **74**: 354–356.
18. Mathew R, Bak TH, Hodges JR. Diagnostic criteria for corticobasal syndrome: a comparative study. *J Neurol Neurosurg Psychiatry* 2012; **83**: 405–410.
19. Murray R, Neumann M, Forman MS et al. Cognitive and motor assessment in autopsy-proven corticobasal degeneration. *Neurology* 2007; **68**: 1274–1283.